Journal of the Optical Society of Korea
Vol. 15, No. 4, December 2011, pp. 345-351
DOI: http://dx.doi.org/10.3807/JOSK.2011.15.4.345

Three-dimensional Binocular Holographic Display Using Liquid Crystal Shutter

Hyun-Eui Kim, Hee-Seung Kim, Kyeong-Min Jeong, and Jae-Hyeung Park*

School of Electrical & Computer Engineering, Chungbuk National University, 410 SungBong-ro, Heungduk-gu, Cheongju 361-763, Korea

(Received July 14, 2011 : revised September 27, 2011 : accepted September 27, 2011)

We present a novel approach to the holographic three-dimensional display using a liquid crystal shutter for binocular display applications. One of the difficult problems in implementing a binocular holographic three-dimensional display is the extremely narrow viewing angle. This problem is attributed to the spatial light modulator pixel number which restricts the maximum spatial bandwidth of the spatial light modulator. In our proposed method, a beam splitter and liquid crystal shutter are used to present two holograms of a three-dimensional scene to the corresponding eyes. The combination of holographic display and liquid crystal shutter can overcome the problem of the extremely narrow viewing angle, presenting three-dimensional images to both eyes with correct accommodation depth cues.

Keywords : Holographic display, Binocular display, Accommodation depth cue
OCIS codes : (090.0090) Holography; (090.1760) Computer holography; (100.6890) Three-dimensional image processing; (110.0110) Imaging systems

I. INTRODUCTION

Three-dimensional (3D) displays can enable us to see natural scenery as it is. Much research has been carried out concerning 3D displays [1-8]. Among them, stereoscopic displays with special glasses or autostereoscopic multi-view displays with a few viewpoints are the representative 3D display technologies being deployed on a commercial scale. These technologies deliver binocular depth cues such as binocular disparity and convergence. However, they do not provide correct accommodation, thus resulting in visual fatigue due to the accommodation-convergence mismatch.

To get around this problem, the holographic 3D display was proposed. The holographic display provides almost perfect depth information by reconstructing the wavefront of the light field [9]. Therefore, the holographic display is free from the above-mentioned problems of conventional stereoscopic and autostereoscopic displays [10]. In spite of its great potential, the current holographic display has many limitations mainly due to the insufficient resolution of the spatial light modulator (SLM). An SLM can modulate the phase of the beam by controlling transparency. Therefore, an SLM can produce the desired wavefronts that eventually produce the desired shape of the object. In order to reconstruct a more complete wave field, the spatial resolution of the SLM should be increased. However, current device technology cannot realize the ultra high resolution SLM required for the holographic 3D display. Due to the insufficient SLM resolution, studies to realize an electro-holographic display face some difficulties such as the narrow viewing angle and small image size.

Various techniques have been proposed to overcome these problems [11]. One common method is to use a horizontal parallax only (HPO) hologram to relieve the SLM resolution requirement. This approach was developed by S. Benton et al. [12]. Their system improves the horizontal viewing angle up to 24 degrees by using an acousto-optic modulator (AOM) and a horizontal scanner array. Y. Takaki et al. enlarge the horizontal viewing angle to 14.6 degrees by using anamorphic projection and a horizontal scanner [13]. Another idea is to arrange multiple SLMs in an array. C. Slinger et al. configured 4 channel active tiling units, delivering 10^8 pixels in an active area [14]. B. Lee et al. arranged multiple SLMs in a circular arc, extending the viewing angle to 22 degrees [15]. Although these previous studies provide a wider viewing

*Corresponding author: jh.park@cbnu.ac.kr
Color versions of one or more of the figures in this paper are available online.

angle, they usually require multiple SLMs or a high speed scanning mechanism with high bandwidth light modulators, which makes the overall system complicated and expensive.

In this paper, we propose a binocular holographic 3D display system using only one SLM. The proposed system configures two optical paths directed to the observer's eyes using a beam splitter. Holograms of the left and right eyes are sequentially presented by SLM, while the liquid crystal (LC) shutters located in two optical paths operate in synchronicity to deliver the displayed holographic 3D image to the corresponding eye. Therefore, the proposed system provides binocular 3D images without causing the accommodation-convergence mismatch problem. Note that the proposed method is different from the previous stereoscopic binocular holographic display techniques [16]. While the previous technique presents a different two-dimensional (2D) image to each eye such that the observer feels depth from binocular disparity, the proposed method presents a different 3D image to each eye such that each eye of the observer sees a 3D images with correct accommodation. Hence, in the proposed method, not only the binocular disparity but also correct accommodation can be presented to the observer. Also note that the proposed method is distinguished from other holographic techniques in that the holograms are used as an image splitting means in place of the parallax barrier or the lenticular lens in conventional multi-view autostereoscopic displays [17-18]. In addition, a technique of enhancing the horizontal viewing angle of the holographic 3D display using only a single SLM has been reported [19]. In this technique, the SLM pixels are spatially reconfigured using specialized optics, sacrificing the vertical bandwidth of the SLM. In contrast, the proposed method uses time multiplexing to present different holographic 3D images to each eye without causing vertical bandwidth reduction. Next, we describe the proposed system and present the experimental results.

II. SYSTEM CONFIGURATION

2.1. Configuration of the Proposed System

The proposed binocular holographic system is configured as shown in Fig. 1. A light source illuminates the SLM that is sequentially loaded with two holographic patterns of different perspectives of a 3D scene, and the reflected light is decoded by a Fourier transform lens. Next to the SLM, two lenses adjust the scale of magnification of the reconstructed 3D image. The light passing through the lenses is divided into two paths by a beam splitter before reaching the image plane where the final 3D image is located. Each split light is

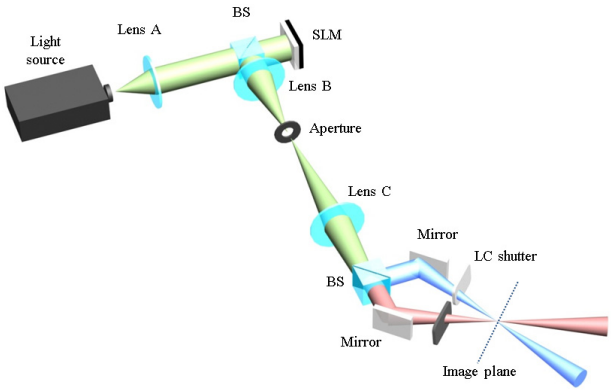

FIG. 1. Schematics of the proposed binocular holographic display.

controlled via a time-multiplexing technique using an LC shutter. Therefore, each reconstructed 3D image containing different perspective is sequentially presented to the corresponding eye.

2.2. Viewing Angle and Image Size of the Reconstructed 3D Image

The viewing angle and size of the image reconstructed by the holographic 3D display are fundamentally limited by the number of pixels of the SLM. Figure 2 shows the optical system used in the proposed display configuration. With a pixel pitch p of SLM, the maximum spatial frequency $f_{x,max}$ that can be represented without aliasing is given by $f_{x,max} = 1/2p$. Since the spatial frequency corresponds to the propagation angle θ and the lateral image location in the Fourier hologram geometry, the maximum image size L_ξ that can be displayed in the aperture plane is

$$L_\xi = 2f\theta_{\max} = 2f\lambda f_{x,\max} = \frac{f\lambda}{p}, \tag{1}$$

where λ is the wavelength, and f is the focal length of the Fourier transform lens (Lens B in Fig. 2). The viewing angle of the reconstructed image in the aperture plane is determined by the numerical aperture of the system as

$$2\varphi = \frac{L_x}{f} = \frac{Np}{f}, \tag{2}$$

where L_x and N are the size and number of pixels of SLM, respectively. From Eqs. (1) and (2), it can be seen that the product of the viewing angle with the maximum image size is limited by $2\varphi\ L_\xi = N\lambda$.

In our configuration, the initial reconstructed image in the aperture plane is magnified by another imaging lens (Lens C

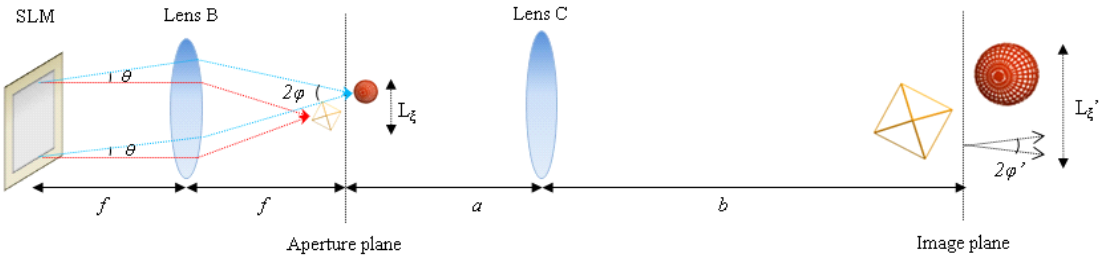

FIG. 2. Optical system of holography reconstruction for a single eye.

in Fig. 2). The size and viewing angle of the final image located in the image plane are given by

$$L'_{\xi} = L_{\xi}\frac{b}{a} = \frac{bf\lambda}{ap}, \tag{3}$$

$$2\varphi' = 2\varphi\frac{a}{b} = \frac{aNp}{bf}, \tag{4}$$

where a and b are distances around the imaging lens. Again, Eqs. (3) and (4) show that the product of image size and viewing angle does not change due to the additional imaging process. In our experimental setup, the final image size and viewing angle are given by L_{ξ}' = 9.98 mm, $2\varphi'$ = 0.49° for 532 nm wavelength, which is sufficient for covering each eye.

2.3. Active LC Shutter Control

The proposed method uses a binocular holographic system for presenting a left holographic image and a right holographic image. Figure 3 shows configuration of the binocular system setup. An active LC shutter control structure is used to deliver the left and right holographic 3D images to the corresponding eyes of the viewer. Figure 4 shows the synchronized operation of the LC shutters and SLM.

The two active LC shutter lenses can be either transparent or opaque by controlling the electrical voltage. The left and right holographic patterns are alternatively displayed on SLM and are synchronized with the electrical voltage of the LC shutter lenses. When SLM is loaded with the hologram pattern of the left eye, the right lens is controlled to be opaque while the left lens is controlled to be transparent. When SLM displays the right image, the glasses lenses are controlled oppositely. Thus, the observer's left or right eye only sees a 3D image reconstructed from the hologram pattern of the corresponding eye on SLM. When the left and right 3D images are switched fast enough, the observer will feel natural single 3D image via the after image effect.

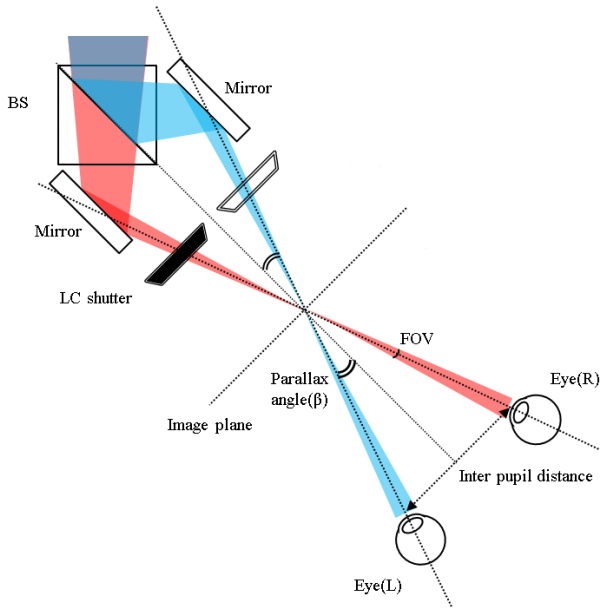

FIG. 3. Schematics of the time division multiplexing system using active LC shutter.

2.4. Rotation Geometry for Left and Right Eye Holography

In the proposed system, two light beams containing the reconstructed 3D image are directed in different directions, i.e., left eye direction and right eye direction. Thus, for a given 3D image, holography for each eye should be created considering the beam direction difference, which eventually results in reconstruction of different perspectives of the 3D image.

Figures 5 and 6 show the geometry of the beam path for the left and right eyes, respectively. Global coordinates (X_G, Y_G, Z_G) are set as shown in Figs. 5 and 6 with the origin located at the crossing point in the image plane of two beams for the left and right eyes. Each point of a desired 3D image is represented by the global coordinates. In the left eye case, the coordinates (X, Y, Z) on SLM are transformed to (X_L, Y_L, Z_L) in the image space as shown in Fig. 5. Angle β in Fig. 5 is given by the converging angle of two eyes of the observer. From the geometry, a point in global coordinates

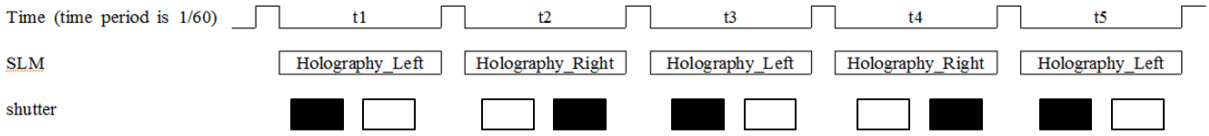

FIG. 4. Active LC shutter control timing.

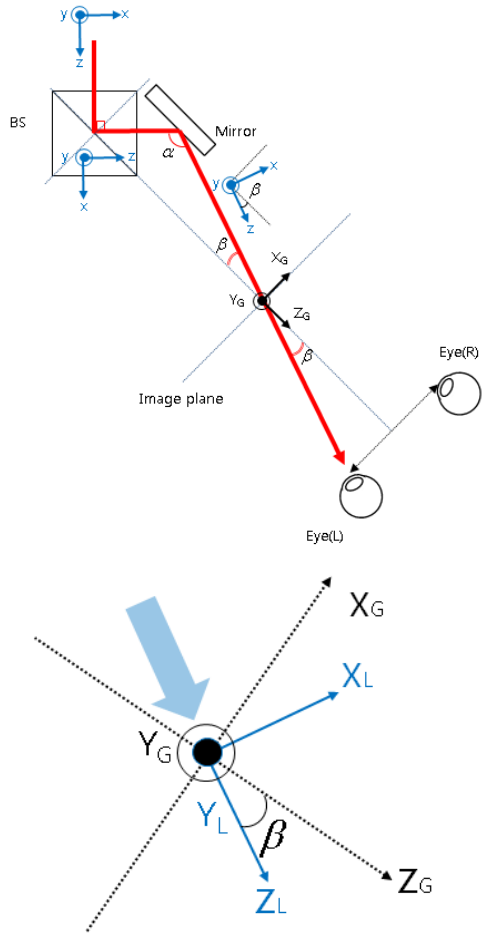

FIG. 5. Rotation of image coordinates for the left eye.

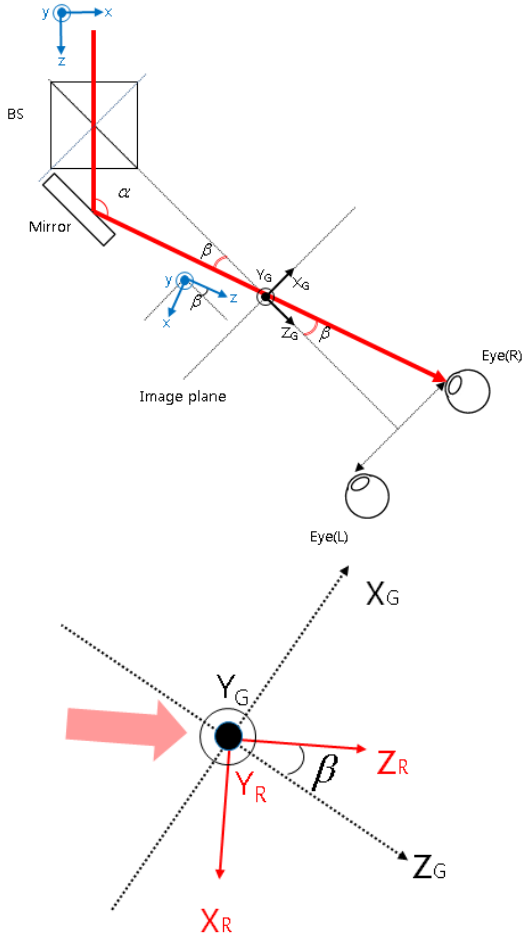

FIG. 6. Rotation of image coordinates for the right eye.

(X_G, Y_G, Z_G) is represented by the (X_L, Y_L, Z_L) coordinates by

$$\begin{pmatrix} x_L \\ y_L \\ z_L \end{pmatrix} = \begin{pmatrix} \sin\beta & 0 & \cos\beta \\ 0 & 1 & 0 \\ \cos\beta & 0 & -\sin\beta \end{pmatrix} \begin{pmatrix} x_G \\ y_G \\ z_G \end{pmatrix}. \quad (5)$$

Similarly, from the geometry of the right eye beam shown in Fig. 6, the point in the same global coordinates (X_G, Y_G, Z_G) is given by the right eye beam coordinates (X_R, Y_R, Z_R) by

$$\begin{pmatrix} x_R \\ y_R \\ z_R \end{pmatrix} = \begin{pmatrix} \sin\beta & 0 & -\cos\beta \\ 0 & 1 & 0 \\ \cos\beta & 0 & \sin\beta \end{pmatrix} \begin{pmatrix} x_G \\ y_G \\ z_G \end{pmatrix}. \quad (6)$$

Note that since the coordinates (X_R, Y_R, Z_R) are left-handed, the sign of X_R value is reversed in Eq. (6). In summary, the points of the 3D image represented in global coordinates are first transformed to left beam coordinates (X_L, Y_L, Z_L) or right beam coordinates (X_R, Y_R, Z_R) using Eqs. (5) and (6), and the left and right holograms are then calculated using data represented by the corresponding coordinates (X_L, Y_L, Z_L) or (X_R, Y_R, Z_R).

2.5. Holography Computation

In the proposed method, the optical configuration of each of the left and right eye beams is that of the Fourier holography [20-21]. Therefore, for a 3D image $U(x_G,y_G,z_G)$, the holography of each eye is calculated by

$$H(x,y)=\frac{1}{j\lambda f}\iiint U(u,v,w)e^{j\phi(u,v,w)}e^{j\frac{\pi w}{\lambda f^2}(x^2+y^2)}e^{j\frac{2\pi}{\lambda f}(xu+yv)}dudvdw, \tag{7}$$

where (u,v,w) is a scaled version of either of (X_L, Y_L, Z_L) or (X_R, Y_R, Z_R), which are transformed from (X_G, Y_G, Z_G) by Eqs. (5) and (6). The phase $\phi(u,v,w)$ is set to be random for each point for higher efficiency.

III. EXPERIMENTAL RESULTS

Figure 7 shows the experimental setup. The SLM used in the experiment is a reflective type phase SLM. The resolution of the SLM is 1920×1080 and the maximum refresh rate is 60Hz. SLM was tested using a Michelson interferometric setup under various input-output polarization states, and the optimum condition was obtained before the SLM was used in the experiment. The LC shutter system used in the experiment has a refresh rate of 120 frames per second (120Hz), so that each eye sees 60 frames per second. Note that the proposed method can be implemented using two discrete LC shutters located in the two beam paths and hence there is no need to wear LC shutter glasses to see the 3D images in the proposed method. In the experiment, we used glasses-type LC shutters as a LC shutter system only because they can be easily obtained. Since the SLM is limited to 60 frames per second (60Hz), the final refresh rate of the implemented binocular holographic system is 30Hz.

The 3D scene used in the experiment is shown in Fig. 8. Note that two holograms for the 3D scene represented in the global coordinates as shown in Fig. 8(a) are calculated after they are transformed to the left and right beam coordinates as shown in Figs. 8(b) and (c). Hence, each hologram reconstructs the same 3D scene but with different perspectives.

First, we verified the optical operation of the LC shutter. Figures 9(a) and (b) show the pictures taken through an LC shutter that is controlled to close and open, respectively. It can be confirmed that the LC shutter transmits or blocks the view as desired. Figure 9(c) shows the picture taken with a different focal plane of the camera, while the LC shutter is maintained open. By comparing Figs. 9(b) and (c), it can be seen that the different part of the displayed 3D image is focused, which confirms that LC layer of the shutter does not destroy the 3D nature of the displayed image in its transparent state.

Then, we verified that accommodation and binocular disparity of the 3D image displayed via the proposed method. The 3D

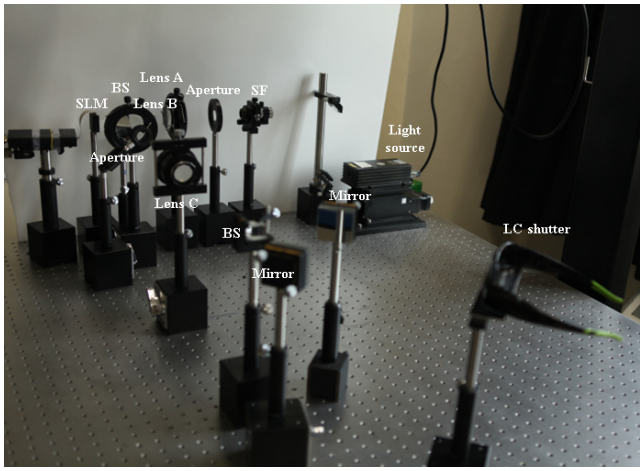

FIG. 7. The experimental setup.

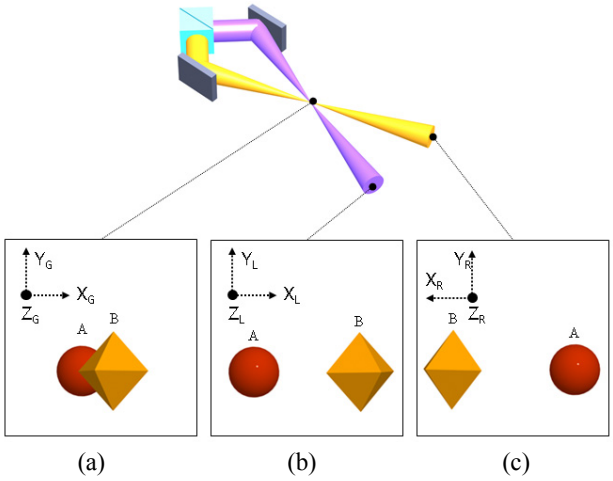

FIG. 8. 3D scene used in the experiment (a) in global coordinates, (b) in coordinates for the left eye, (c) in coordinates for the right eye.

scene shown in Fig. 8 is displayed and two reference objects A' and B' are located where two parts A and B of the 3D scene are displayed. Figures 10(a) and (b) show the pictures taken with different camera focal planes for the right eye view. It can be seen that the 3D images A and B and the reference objects A' and B' are focused at different focal distances as expected. The same result can be observed for the left eye views as well, as shown in Figs. 10(c) and (d). From this observation, it is confirmed that the proposed system can correctly provide the accommodation. Moreover, it can also be observed by comparing Figs. 10(a) and (c) that the displayed 3D images A and B are exactly above the reference objects A' and B', though the viewing direction is altered from right to left view. This means that the location of displayed 3D images in the global coordinates is maintained in the reconstruction of left and right view holograms. Hence,

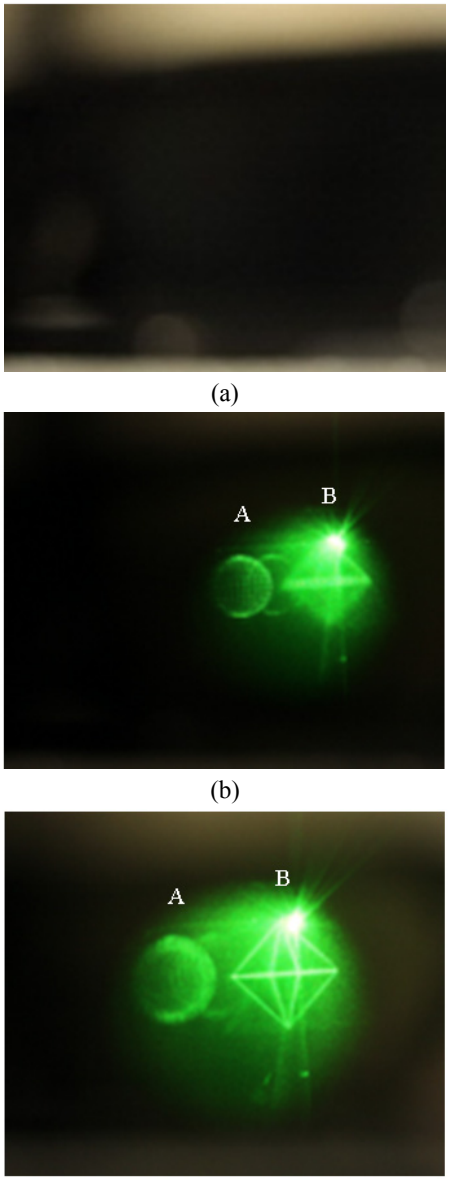

(a) (b) (c)

FIG. 9. Transmission of the displayed 3D image in different LC shutter states (a) opaque state, (b) transparent state, (c) transparent state with a different camera focal distance.

binocular disparity is also correctly delivered by the proposed method. From the above observations, it can be confirmed that the proposed method can correctly provide both of the accommodation and binocular disparity, eliminating accommodation-convergence mismatch problem of the conventional 3D displays.

IV. CONCLUSION

In this paper, a novel binocular holographic 3D display

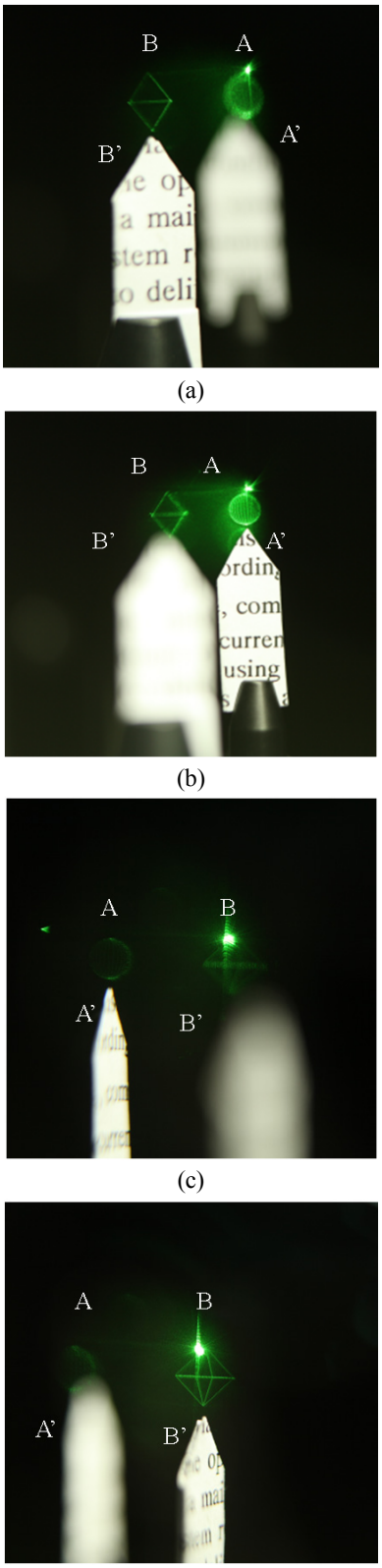

(a) (b) (c) (d)

FIG. 10. Reconstruction result of a 3D scene. Right eye view with the camera focal plane at (a) Z_G = 10mm, and (b) Z_G = -10mm. Left eye view with the camera focal plane at (c) Z_G = 10 mm, and (d) Z_G = -10mm.

system is proposed. We have combined a time division multiplexing system using an LC shutter with a holographic 3D display system in order to deliver 3D images to both eyes of the observer. Binocular holographic reconstruction ensures that both of the accommodation and binocular disparity are provided, relieving the accommodation-convergence mismatch problem of the conventional 3D displays. The time multiplexing scheme enables the implementation of the system using only one SLM by eliminating the necessity to enlarge the static viewing angle of the holographic reconstruction.

ACKNOWLEDGMENT

This research was partly supported by Basic Science Research Program through the National Research Foundation of Korea (NRF) funded by the Ministry of Education, Science and Technology (2011-0003395). This work was also partly supported by the IT R&D program of MKE/KEIT. [KI001810035337, A development of interactive wide viewing zone SMV optics of 3D display]

REFERENCES

1. A. R. L. Travis, "Autostereoscopic 3-D display," Appl. Opt. **29**, 4341-4342 (1990).
2. B. Lee, J.-H. Park, and S.-W. Min, "Three-dimensional display and information processing based on integral imaging," in *Digital Holography and Three-dimensional Display*, T.-C. Poon, ed. (Springer, New York, USA, 2006), pp. 333-378.
3. A. Kubota, A. Smolic, M. Magnor, M. Tanimoto, and T. Chen, "Multiview imaging and 3DTV," IEEE Signal Processing Magazine **24**, 10-21 (2007).
4. P. Benzie, J. Watson, P. Surman, I. Rakkolainen, K. Hopf, H. Urey, V. Sainov, and C. von Kopylow, "A survey of 3DTV displays: techniques and technologies," IEEE Trans. Circuits Syst. Video Technol. **17**, 1647-1658 (2007).
5. S.-W. Min, B. Javidi, and B. Lee, "Enhanced three-dimensional integral imaging system by use of double display devices," Appl. Opt. **42**, 4186-4194 (2003).
6. J.-H. Park, K. Hong, and B. Lee, "Recent progress in three-dimensional information processing based on integral imaging," Appl. Opt. **48**, H77-H94 (2009).
7. T.-G. Kim and Y.-S. You, "Extraction of a distance parameter in optical scanning holography using axis transformation," J. Opt. Soc. Korea **14**, 104-108 (2010).
8. S.-H. Jeon and S.-K. Gil, "Qpsk modulation based optical image cryptosystem using phase-shifting digital holography," J. Opt. Soc. Korea **14**, 97-103 (2010).
9. H. Kim, J. Hahn, and B. Lee, "Mathematical modeling of triangle-mesh-modeled three-dimensional surface objects for digital holography," Appl. Opt. **47**, D117-D127 (2008).
10. S. Reichelt, R. Haussler, G. Futterer, and N. Leister, "Depth cues in human visual perception and their realization in 3D displays," Proc. SPIE **7690**, 7690 0B (2010).
11. F. Yaras, H. Kang, and L. Onural, "State of the art in holographic displays: a survey," J. Display Technology **6**, 443-454 (2010).
12. T. A. Nwodoth and S. A. Benton, "Chidi holographic video system," Proc. SPIE **3596**, 167-176 (2000).
13. Y. Takaki and Y. Hayashi, "Increased horizontal viewing zone angle of a hologram by resolution redistribution of a SLM," Appl. Opt. **47**, D6-D11 (2008).
14. M. Stanley, M. A. Smith, A. P. Smith, P. J. Watson, S. D. Coomber, C. D. Cameron, C. W. Slinger, and A. D. Wood, "3D electronic holography display system using a 100 mega-pixel spatial light modulator," Proc. SPIE **5249**, 297-308 (2004).
15. J. Hahn, H. Kim, Y. Lim, G. Park, and B. Lee, "Wide viewing angle dynamic holographic stereogram with a curved array of spatial light modulators," Opt. Express **16**, 12372-12386 (2008).
16. S.-H. Lee and E.-S. Kim, "Stereoscopic display based on a volume holographic storage," Japan J. Appl. Phys. **37**, L1193-L1194 (1998).
17. S.-H. Lee, H.-G. Yang, K.-C. Son, and E.-S. Kim, "Multiviewpoint autostereoscopic display system based on volume hologram," Proc. SPIE **3957**, 208-214 (2000).
18. W.-C. Su, C.-Y. Chen, and Y.-F. Wang, "Stereogram implemented with a holographic image splitter," Opt. Express **19**, 9942-9949 (2011).
19. H.-J. Kang, N. Ohmura, T. Yamaguchi, H. Yoshikawa, S.-C. Kim, and E.-S. Kim, "Method to enlarge the hologram viewing window using a mirror module," Opt. Eng. **48**, 075801-1~075801-7 (2009).
20. J. H. Park, M. S. Kim, G. Baasantseren, and N. Kim, "Fresnel and Fourier hologram generation using orthographic projection images," Opt. Express **17**, 6320-6334 (2009).
21. M. S. Kim, G. Baasantseren, N. Kim, and J. H. Park, "Hologram generation of 3D objects using multiple orthographic view images," J. Opt. Soc. Korea **12**, 269-274 (2008).